Molecular Structure and Conformational Analysis of 1-Phenyl-1-X-1-Silacyclohexanes (X = F, Cl) by Electron Diffraction, Low-Temperature NMR, and Quantum Chemical Calculations

Bagrat A. Shainyan,*,[†] Alexander V. Belyakov,*,[‡] Yurii F. Sigolaev,[‡] Alexander N. Khramov,[‡] and Erich Kleinpeter*,[§]
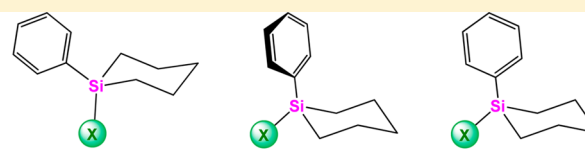
[†]A. E. Favorsky Irkutsk Institute of Chemistry, Siberian Division of the Russian Academy of Science, 1 Favorsky Street, 664033 Irkutsk, Russian Federation

[‡]St. Petersburg State Technological Institute, 190013 St. Petersburg, Russia

[§]Chemisches Institut der Universitat Potsdam, Karl-Liebknecht-Straße 24-25, D-14476 Potsdam (Golm), Germany

Ⓢ *Supporting Information*

ABSTRACT: The molecular structure and conformational preferences of 1-phenyl-1-X-1-silacyclohexanes $C_5H_{10}Si(Ph,X)$ (X = F (**3**), Cl (**4**)) were studied by gas-phase electron diffraction, low-temperature NMR spectroscopy, and high-level quantum chemical calculations. In the gas phase only three (**3**) and two (**4**) stable conformers differing in the axial or equatorial location of the phenyl group and the angle of rotation about the $Si-C_{Ph}$ bond (ax_i and ax_o denote the Ph group lying in or out of the $X-Si-C_{Ph}$ plane) contribute to the equilibrium. In **3** the ratio $Ph_{eq}:Ph_{axo}:Ph_{axi}$ is 40(12):55(24):5 and 64:20:16 by experiment and theory, respectively. In **4** the ratio $Ph_{eq}:Ph_{axo}$ is 79(15):21(15) and 71:29 by experiment and

		Ph_{eq}	Ph_{ax_o}	Ph_{ax_i}
GED	X = F	40	55	5
	X = Cl	79	21	–
M06-2X	X = F	64	20	16
	X = Cl	71	29	–
LT NMR	X = F	76	24	
	X = Cl	82	18	

theory (M06-2X calculations), respectively. The gas-phase electron diffraction parameters are in good agreement with those obtained from theory at the M06-2X/aug-ccPVTZ and MP2/aug-cc-pVTZ levels. Unlike the case for M06-2X, MP2 calculations indicate that **3**-Ph_{eq} conformer lies 0.5 kcal/mol higher than the **3**-Ph_{axo} conformer. As follows from QTAIM analysis, the phenyl group is more stable when it is located in the axial position but produces destabilization of the silacyclohexane ring. By low-temperature NMR spectroscopy the six-membered-ring interconversion could be frozen at 103 K and the present conformational equilibria of **3** and **4** could be determined. The ratio of the conformers is **3**-Ph_{eq}:**3**-Ph_{ax} = (75−77):(23−25) and **4**-Ph_{eq}:**4**-Ph_{ax} = 82:18.

■ INTRODUCTION

Silacyclohexanes and silaheterocyclohexanes, because of specific structural features such as longer $Si-C$ vs $C-C$ bonds and a smaller degree of folding of the silicon part of the molecule, demonstrate conformational preferences principally different from those of their carbon analogues. Of particular interest are the effects of 1-substituents at silacyclohexane[1] and the influence of additional heteroatoms (X = O, S, NR) concerning synthesis and conformational analysis of silaheterocyclohexanes, especially in silacyclohexanes and silaheterocyclohexanes geminally disubstituted at silicon.[2]

The structurally and conformationally investigated 1,1-disubstituted 1-silacyclohexanes $C_5H_{10}SiXY$ (**1**) are so far limited to five pairs of substituents X and Y: Me, F;[3] Me, Cl;[4] Me, CF_3;[3] Cl, $SiCl_3$;[5] and Me, Ph.[2]
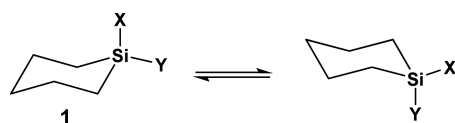

The analogues of **1**, 3,3-disubstituted 1-aza(oxa,thia)-3-silacyclohexanes ZC_4H_8SiXY (**2**), have also been synthesized and studied, such as azasilacyclohexanes (**2**, Z = NR; X, Y = Ph, Me;[6,7] X, Y = Me, OR^8), oxasilacyclohexanes (**2**, Z = O; X, Y = Ph, Me;[9] X, Y = Me, OR^{10}), and thiasilacyclohexanes (**2**, Z = S; X, Y = Ph, Me;[2] X, Y = Me, F[11]).
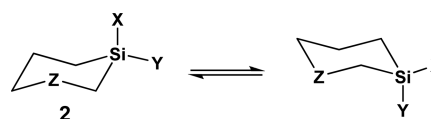

No data are available on compounds of type **1** or **2** simultaneously containing a phenyl group and an electronegative atom at silicon. Such a combination is of particular interest because of (i) the drastic decrease in the conformational energy of the phenyl group at silicon in comparison to
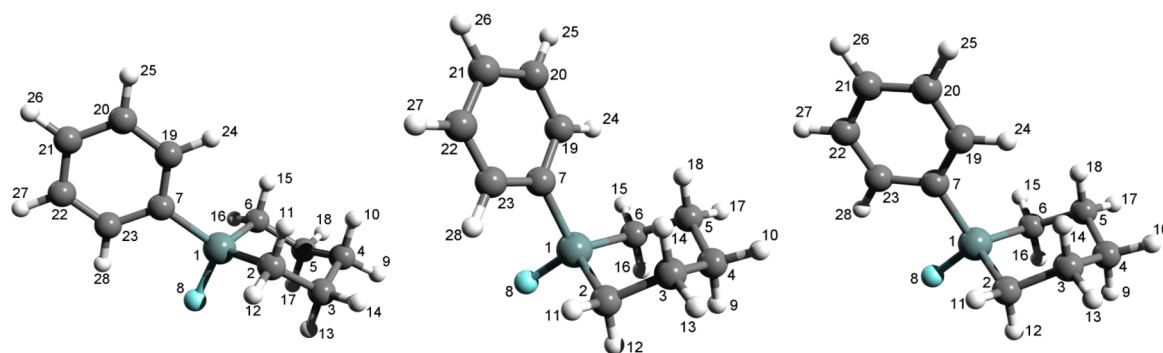
Figure 1. Molecular models of the Ph$_{eq}$ (left), Ph$_{axo}$ (center), and Ph$_{axi}$ (right) conformers of molecules **3** and **4** with atom numbering. Atom 8 is fluorine (**3**) or chlorine (**4**).
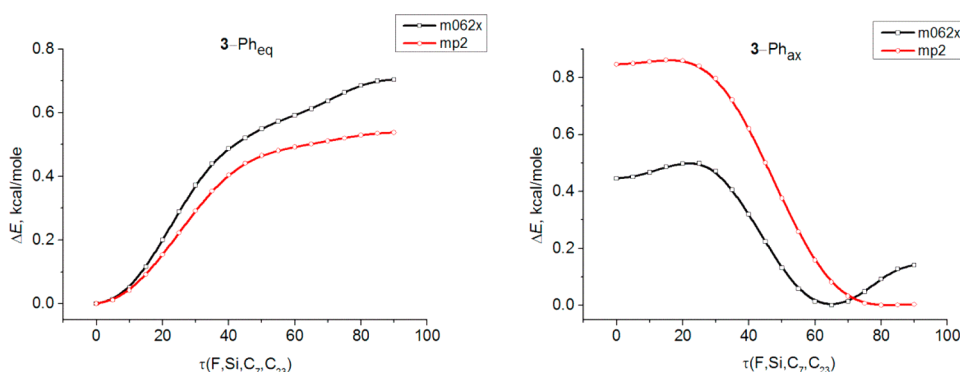
Figure 2. Potential energy profiles of the phenyl group rotation about the Si−C7 bond for the equatorial and axial positions of compound **3** at the M06-2X/aug-cc-pvTZ and MP2/cc-pvTZ levels of theory.

that at carbon,[2] (ii) the strong axial preference of electronegative groups at silicon,[12−17] and (iii) the axial preference of the phenyl group in the geminally disubstituted carbon analogue of **1**, 1-methyl-1-phenylcyclohexane.[18,19]

Recently, we have synthesized and characterized 1-phenyl-1-X-1-silacyclohexanes C$_5$H$_{10}$Si(X)Ph (X = F (**3**), Cl (**4**), Br (**5**)).[20] While the bromo derivative **5** turned out to be very unstable, the two other compounds were successfully isolated and purified. Herein we present the results of combined theoretical and experimental studies of compounds **3** and **4** using gas-phase electron diffraction, very low temperature ^{13}C NMR, and high-level quantum chemical calculations.

■ EXPERIMENTAL SECTION

Theoretical Calculations. Quantum chemical calculations were performed with the Gaussian 09 program suite[21] at up to M06-2X/aug-cc-pVTZ and MP2/aug-cc-pVTZ levels of theory. Topological analyses of electron density were performed with the use of the AIM method.[22] Noncovalent interaction (NCI) analysis of electron density[23] including positions of the noncovalent interactions in real space and decoupling of the involved balance of interactions that defines such interactions was done with the NCIPLOT program.[24] Chemical shifts were calculated for all conformers of compounds **3** and **4** at the GIAO/B3LYP/cc-pVTZ and GIAO/MP2/6-311+G(d,p) levels of theory on the geometry optimized at the MP2/aug-cc-pVTZ level for **3** and MP2/cc-pVTZ level for **4**.

Gas-Phase Electron Diffraction. The purity of samples **3** and **4** prepared as described in ref 20 according to ^{1}H NMR was better than 98%. The combined gas-phase electron diffraction and mass spectrometric experiment, GED/MS,[25−27] was carried out in the ISUCT on the EMR-100M apparatus using the R^3 sector. The optical densities of the diffraction patterns were measured by a computer-controlled MD-100 (Carl Zeiss, Jena, Germany) microdensitometer.[28]

The molecular scattering function, $sM(s)$, was evaluated as $sM(s) = (I_t(s)/I_b(s) - 1)s$, where $I_t(s)$ is the total electron scattering intensity and $I_b(s)$ is the experimental background. After it crossed the fast electron beam in the diffraction chamber, the molecular beam from the effusion cell entered directly the ionization chamber of a monopole mass spectrometer attached to the GED unit. This allowed real-time monitoring of the vapor composition by recording the mass spectra simultaneously with recording of the diffraction patterns. Information about the experimental conditions for all data sets used in the present investigation is given in Table S1 in the Supporting Information. The atomic scattering factors were taken from ref 29.

The algorithm described in ref 30 was used to calculate Cartesian coordinates of atoms. For the ring closure the calculation of the coordinates was not terminated at the last atom in the ring but continued for the three dummy atoms as described in ref 30. The problem of ring closure reduces to the iterative solution of nonlinear equations with respect to the dependent geometrical parameters so that Cartesian coordinates of dummy atoms coincide with those of the first three atoms of the ring. The minimized functional for refining structural parameters has the form

$$Q = \sum_s w_s \Delta_s^2 = \sum_s w_s [sM^{obs}(s) - k \cdot sM^{calc}(s)]^2$$

where w_s is a weight function, $s = (4\pi/\lambda)\sin(\theta/2)$ is the scattering parameter for angle θ, λ is the wavelength of the electron beam, $sM(s)$ is the molecular intensity function, and k is the scale factor. The value for the R factor serves as a criterion of the minimum of the functional:

$$R = (Q/\sum_s w_s [sM^{obs}(s)]^2)^{1/2}$$

Least-squares structure refinements were carried out with a modified version of the KCED25 program.[31,32] Weight matrices were diagonal. The short-distance data were assigned weights of 0.5 and the long-distance data were assigned weights of unity. Estimated standard deviations calculated by the program were multiplied by a
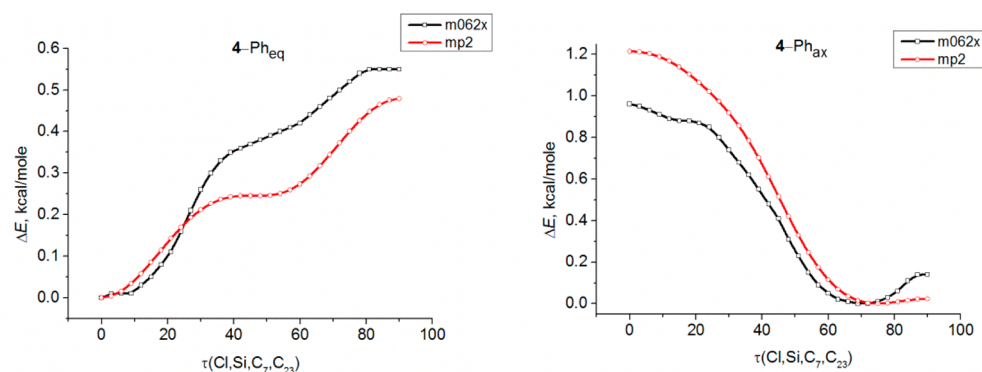
Figure 3. Potential energy profiles of the phenyl group rotation about the Si−C7 bond for the equatorial and axial positions of compound **4** at the M06-2X/cc-pvTZ and MP2/cc-pvTZ levels of theory.

Table 1. Selected Calculated (with Basis Set aug-cc-pVTZ) and Experimental (GED) Geometrical Parameters, Relative Energies, and Mole Fractions for Conformers 3-Ph$_{eq}$ and 3-Ph$_{axo}$ [a]

param	3-Ph$_{eq}$			3-Ph$_{axo}$		
	M06-2X	MP2	exptl	M06-2X	MP2	exptl
			Bond Distances (Å)			
Si−F	1.619	1.627	1.619(9)	1.615	1.623	1.614(9)
Si−C2	1.864	1.869	1.859(16)	1.863	1.868	1.859(16)
C2−C3	1.539	1.539	1.539(23)	1.540	1.541	1.540(28)
C3−C4	1.531	1.531	1.531(23)	1.531	1.531	1.531(28)
Si−C7	1.862	1.866	1.857(16)	1.868	1.872	1.864(16)
C7−C23	1.396	1.403	1.408(18)	1.398	1.404	1.410(18)
C23−C22	1.389	1.394	1.401(18)	1.387	1.394	1.399(18)
C21−C22	1.387	1.394	1.400(18)	1.389	1.394	1.401(18)
C20−C21	1.389	1.395	1.401(18)	1.387	1.394	1.399(18)
C20−C19	1.387	1.393	1.399(18)	1.389	1.394	1.401(18)
C7−C19	1.398	1.404	1.410(18)	1.396	1.403	1.404(18)
C−H$_{av}$	1.095	1.096	1.095(5)	1.095	1.096	1.095(5)
C$_{Ph}$−H$_{av}$	1.085	1.086	1.085(5)	1.085	1.086	1.085(5)
			Bond Angles (deg)			
Si−C2−C3	110.4	110.5	111.2(3.1)	109.1	108.3	110.0(3.1)
C2−C3−C4	113.3	113.1	114.2(3.1)	113.2	113.1	114.2(3.1)
C3−C4−C5	114.0	113.9	114.9(3.1)	114.2	114.2	115.0(3.1)
C2−Si−C6[b]	105.6	105.4	107.1	105.7	105.2	105.8
C2−Si−F	108.0	108.2	107.3(5.2)	109.5	110.8	108.8(5.2)
C2−Si−C7	114.3	114.0	114.5(4.0)	111.0	109.9	111.2(4.0)
C23−C7−Si[c]	121.3	121.7	121.3	120.0	120.7	120.0
C22−C23−C7	120.9	120.8	120.8(9)	121.2	121.2	121.2(9)
C21−C22−C23	120.0	120.1	120.0(9)	119.9	119.9	119.8(9)
C20−C21−C22	119.9	119.9	119.9(9)	119.9	119.8	119.9(9)
C19−C20−C21[b]	119.8	119.9	120.0	119.9	119.9	120.0
C7−C19−C20[b]	121.1	121.1	120.9	121.2	121.2	121.0
C23−C7−C19[b]	118.3	118.3	118.4	118.0	117.9	118.1
			Dihedral Angles (deg)			
Si−C2−C3−C4	55.3	55.4	53(8)	−57.0	−57.8	−55 (8)
C2−C3−C4−C5	−66.2	−66.8	−66.2[c]	66.7	66.4	67(8)
C2−Si−C6−C5[b]	44.1	43.7	35.8	−46.8	−48.5	−42.5
F−Si−C7−C23	0.0	0.0	0.0[c]	66.0	73.4	65(17)
			Relative Energies and Mole Fractions			
ΔE (kcal/mol)	0.0	0.5		0.3	0.0	
ΔG° (kcal/mol)	0.0		0.2(3)	0.7		0.0(3)
χ (%)	64		40(14)	20		55(24)

[a]For atom numbering see Figure 1. r_e and $\angle_e$ values (calculations) and r_a and $\angle_{h1}$ values (GED) are given. Values in parentheses are 3σ. Bond angles with H atoms were fixed on calculated values. R factor 4.2%. [b]Dependent parameter. [c]Fixed values.

factor of 3 to include added uncertainty due to data correlation and an estimated scale uncertainty of 0.1%.[33]

Low-Temperature NMR Measurements. The low-temperature ^{13}C NMR spectra were recorded at 150.95 MHz in a solvent mixture

Table 2. Selected Calculated (with Basis Set aug-cc-pVTZ) and Experimental (GED) Geometrical Parameters, Relative Energies, and Mole Fractions for Conformers 4-Ph$_{eq}$ and 4-Ph$_{axo}$[a]

param	4-Ph$_{eq}$			4-Ph$_{axo}$		
	M06-2X	MP2	exptl	M06-2X	MP2	exptl
			Bond Distances (Å)			
Si−Cl	2.089	2.084	2.080(4)	2.084	2.079	2.075(4)
Si−C2	1.868	1.872	1.863(9)	1.867	1.870	1.862(9)
C2−C3	1.537	1.537	1.540(20)	1.539	1.539	1.542(20)
C3−C4	1.531	1.530	1.534(20)	1.531	1.531	1.534(20)
Si−C7	1.866	1.868	1.861(9)	1.869	1.870	1.864(9)
C7−C23	1.395	1.402	1.404(8)	1.397	1.404	1.406(8)
C23−C22	1.389	1.394	1.398(8)	1.386	1.393	1.395(8)
C21−C22	1.387	1.393	1.396(8)	1.389	1.394	1.398(8)
C20−C21	1.389	1.394	1.398(8)	1.387	1.393	1.396(8)
C20−C19	1.387	1.393	1.396(8)	1.389	1.394	1.398(8)
C7−C19	1.399	1.405	1.408(8)	1.395	1.403	1.404(8)
C−H$_{av}$	1.093	1.093	1.095(6)	1.093	1.093	1.095(6)
C$_{Ph}$−H$_{av}$	1.082	1.082	1.084(6)	1.082	1.082	1.084(6)
			Bond Angles (deg)			
Si−C2−C3	110.5	110.4	110.8(8)	108.9	108.5	109.3(8)
C2−C3−C4	113.3	113.2	113.8(8)	113.2	113.1	113.8(8)
C3−C4−C5	114.1	114.1	114.4(8)	114.2	114.2	114.5(8)
C2−Si−C6[b]	105.4	105.1	106.9	105.5	105.0	106.1
C2−Si−Cl	107.6	107.8	108.3(1.6)	109.5	110.3	110.2(1.6)
C2−Si−C7	113.8	113.7	112.8(2.2)	111.0	110.3	110.0(2.2)
C23−C7−Si	123.6	123.5	123.4(1.8)	120.1	120.3	119.9(1.8)
C22−C23−C7	120.8	120.8	121.0(6)	121.1	121.1	121.3(6)
C21−C22−C23	120.1	120.2	120.3(6)	119.9	119.9	120.1(6)
C20−C21−C22	119.9	119.8	120.1(6)	119.9	119.9	120.1(6)
C19−C20−C21[b]	119.8	119.9	118.7	119.9	120.0	118.8
C7−C19−C20[b]	121.1	121.1	122.6	121.0	121.0	122.6
C23−C7−C19[b]	118.3	118.3	117.2	118.2	118.1	117.1
			Dihedral Angles (deg)			
Si−C2−C3−C4	55.2	55.6	53(2)	−57.3	−58.0	−56(2)
C2−C3−C4−C5[c]	−66.2	−66.6	−66.2	66.6	66.8	66.6
C2−Si−C6−C5[b]	43.8	44.2	40.1	−46.4	−47.7	−45.3
Cl−Si−C7−C23[c]	0.0	0.0	0.0	66.0	73.4	75.0
			Relative Energies and Mole Fractions			
ΔE (kcal/mol)	0.0	0.0		0.7	0.3	
ΔG° (kcal/mol)	0.0		0.0(4)	0.5		0.8(4)
χ (%)	71		79(15)	29		21(15)

[a]For atom numbering see Figure 1. r_e and ∠$_e$ values (calculations) and r_a and ∠$_{h1}$ values (GED) are given. Values in parentheses are 3σ. Bond angles with H atoms were fixed on calculated values. *R* factor 5.8%. [b]Dependent parameter. [c]Fixed values.

of CD$_2$Cl$_2$, CHFCl$_2$, and CHF$_2$Cl in a ratio of 1:1:3. Standard software was employed for both acquisition (AQ = 0.91 s; relaxation delay 2 s; 64K digital points; power gated; 30° pulse angle −90°; 9.7 μs) and processing (window function: exponential multiplication with 1 Hz line broadening factor). The probe temperature was calibrated by means of a thermocouple inserted into a dummy tube. The low-temperature measurements were estimated to be accurate to ±2 K. The conformer ratio was determined by integration of the separated signals in the frozen spectrum (cf. Figures 8 and 9).

■ RESULTS

Molecular Structure. The geometries of the conformers were optimized without symmetry restrictions; for atom numbering in molecules **3** and **4**, see Figure 1. The correlation of the stationary points on the potential energy surface to minima was proved by the absence of imaginary frequencies in normal mode calculations.

The phenyl group is an asymmetric rotor; therefore, its rotation about the Si−C7 bond may result in the appearance of

several conformers. The corresponding potential energy profiles are presented in Figures 2 and 3. For the **3**-Ph$_{eq}$ and **4**-Ph$_{eq}$ conformers both methods give the minimum for the rotamers with the phenyl ring plane bisecting the C2−Si−C6 angle of the silacyclohexane ring. For the **3**-Ph$_{ax}$ and **4**-Ph$_{ax}$ conformers, the minimum energy rotamers about the C7−Si bond have a skewed conformation with a X−Si−C7−C23 dihedral angle of ∼70° (Figures 2 and 3). However, a very shallow (<0.06 kcal/mol) minimum corresponding, as in the case of the Ph$_{eq}$ conformers, to the rotamers with the phenyl ring plane bisecting the C2−Si−C6 angle of the silacyclohexane ring was located for molecule **3** (Figure 2).

Electron Diffraction. The refined set of geometrical parameters is shown in Tables 1 and 2. The subscripts ax*i* and ax*o* denote the Ph group lying in or out of the X−Si−C$_{Ph}$ plane. The Ph$_{eq}$ and Ph$_{axi}$ conformers have C$_s$ symmetry, and the Ph$_{axo}$ conformers have C$_1$ symmetry. The final molecular
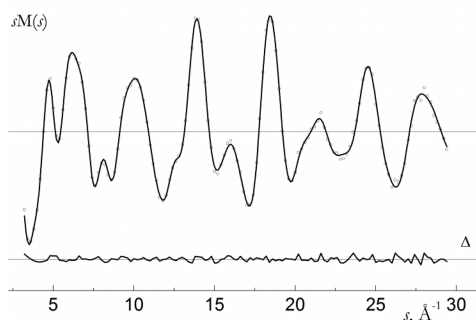
intensity $sM(s)$ and radial distribution $f(r)$ curves are given in Figures 4–7.
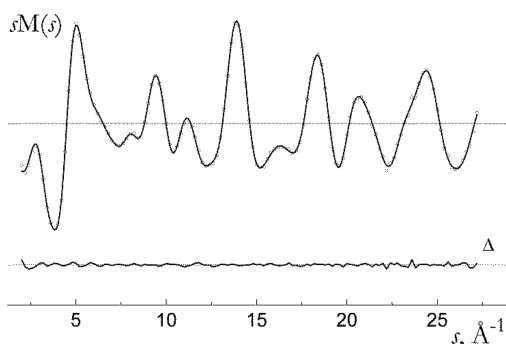
Figure 4. Experimental (dots) and calculated (solid line) molecular intensity curves $sM(s)$ for compound **3**. Below the difference curve Δ for the GED set of parameters from Table 1 is given.
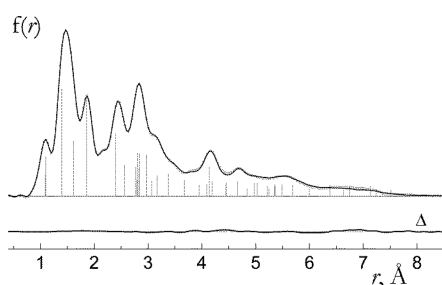
Figure 5. Experimental (dots) and calculated (solid lines) radial distribution curves $f(r)$ for compound **3**. Below the difference curve Δ for the GED set of parameters from Table 1 is given.
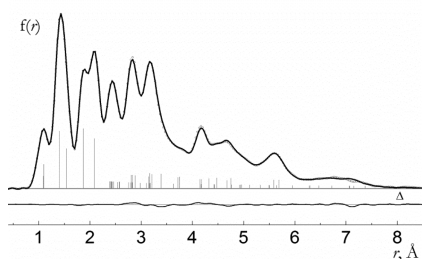

Figure 6. Experimental (dots) and calculated (solid line) molecular intensity curves $sM(s)$ for compound **4**. Below the difference curve Δ for the GED set of parameters from Table 2 is given.

Figure 7. Experimental (dots) and calculated (solid lines) radial distribution curves $f(r)$ for compound **4**. Below the difference curve Δ for the GED set of parameters from Table 2 is given.

Bond angles with hydrogen atoms were fixed at calculated values. The structure of the benzene ring deviates from a regular hexagon. The small differences between similar geometric parameters were constrained at the values calculated at the M06-2X level (Tables 1 and 2). M06-2X theoretical force constants were used to calculate mean vibrational amplitudes (u_{ij}) and shrinkage corrections ($r_{h1} - r_a$) necessary for GED analysis using the SHRINK computer program.[34,35] Geometrical parameters and vibrational amplitudes were refined in groups with constant differences from theoretical calculations. Selected theoretical and experimental root-mean square vibration amplitudes and vibration corrections are shown in Tables 3 and 4.

Dynamic NMR. As it is necessary to determine for substituted silacyclohexanes and silaheterocyclohexanes in solution both the barrier to six-membered-ring interconversion and the position of the appropriate conformational equilibrium,[36] solutions of compounds **3** and **4** in a Freon mixture (CD_2Cl_2:$CHFCl_2$:CHF_2Cl = 1:1:3) were studied to very low temperatures in our special probehead for temperature-dependence studies down to 98 K. The results are given in Figures 8 and 9. For compound **3**, the coalescence temperature T_c (temperature of most advanced line broadening) of the ring interconversion can be assigned as 105 K (Figure 8). Thus, the barrier to six-membered-ring interconversion proves to be at the lowest temperature border where dynamic processes can still be estimated (4–6 kcal/mol). The more exact measurement of the related $\Delta G^{\ddagger}$ parameter cannot be achieved because (i) the lowest temperature to accomplish, (ii) decoalescence not yet being complete at 98 K, and (iii) the ratio of the participating conformers proving to be quite different. The not yet completed decoalescence of related signals also bedevils the precise identification of the free energy difference $\Delta G°$ of the participating conformers. In addition, there are impurity signals at the position of the minor conformer which additionally at incomplete decoalescence complicates comprehensible integration. If the small signal at high field for C-4 at ca. 27.8 ppm is used as a more or less reliable notification of the impurity integration (ca. 9 su), a ratio of the conformers of 3-Ph_{eq}:3-Ph_{ax} = (75−77):(23−25) can be estimated. This result is in complete agreement with previously determined barriers to six-membered-ring interconversions,[2] (H(ax)/Me(eq)):(H-(eq)/Me(ax)) = 74:26,[37] (H(ax)/Ph(eq)):(H(eq)/Ph(ax)) = 78:22,[2] and (Me(ax)/Ph(eq)):(Me(eq)/Ph(ax)) = (62−64):(36−38),[2] and the fact that F and Cl as substituents at silicon prefer the axial orientation: (H(ax)/F(eq)):(H(eq)/F(ax)) = 36:64[16] and (H(ax)/Cl(eq)):(H(eq)/Cl(ax)) = 35:65.[17]

Compound **3**, due to the preferred axial orientation of the fluorine atom, better than that of methyl in this position in 1-methyl-1-phenylsilacyclohexane, assists the equatorial preference of the phenyl substituent at silicon and shifts the conformational equilibrium by increasing the amount of the 3-Ph_{eq} conformer to 75−77%.

Finally, the conformational analysis of compound **4** excellently fits in from low-temperature ^{13}C NMR spectra (Figure 9); a similar low barrier to ring interconversion (ca. 4−6 kcal/mol) can be concluded. Within the lowest temperature spectrum at 103 K (no lock but only broadening at 98 K) only the signal of C-3,5 can be studied, and its integration gives the ratio 4-Ph_{eq}:4-Ph_{ax} = 82:18. The fraction of the Ph_{eq} conformer in **4** further increases in comparison to **3** because the chlorine atom prefers the axial position even more than does the fluorine atom[17] and supports the phenyl substituent at silicon

Table 3. Selected Theoretical (M06-2X) and Experimental (GED) Root Mean Square Vibration Amplitudes u and Vibration Corrections ($r_a - r_{h1}$) for 3-Ph$_{eq}$ and 3-Ph$_{ax}$ [a]

| | 3-Ph$_{eq}$ | | | 3-Ph$_{ax}$ | | |
| | u (Å) | | | u (Å) | | |
param	theor	GED	$r_a - r_{h1}$ (Å)	theor	GED	$r_a - r_{h1}$ (Å)
Si−F	0.043	0.043(4)	0	0.042	0.043(4)	0
Si−C2	0.052	0.053(3)	0.001	0.052	0.052(3)	0.001
C2−C3	0.052	0.052(4)	0.001	0.052	0.053(4)	0.001
C3−C4	0.051	0.052(4)	0	0.051	0.052(4)	0
Si−C7	0.050	0.051(3)	0	0.051	0.052(3)	0
C7−C23	0.046	0.046(4)	0.001	0.046	0.046(4)	0.001
C23−C22	0.045	0.046(4)	0	0.045	0.045(4)	0
C2−H	0.077	0.078(4)	0.002	0.077	0.078(4)	0.02

[a]Vibrational corrections lower than 0.001 are displayed as 0.

Table 4. Selected Theoretical (M06-2X) and Experimental (GED) Root Mean Square Vibration Amplitudes u and Vibration Corrections ($r_a - r_{h1}$) for 4-Ph$_{eq}$ and 4-Ph$_{ax}$ [a]

| | 4-Ph$_{eq}$ | | | 4-Ph$_{ax}$ | | |
| | u (Å) | | | u (Å) | | |
param	theor	GED	$r_a - r_{h1}$ (Å)	theor	GED	$r_a - r_{h1}$ (Å)
Si−Cl	0.050	0.052(3)	0	0.050	0.051(3)	0
Si−C2	0.052	0.053(3)	0.001	0.052	0.053(3)	0.001
C2−C3	0.052	0.053(3)	0.001	0.052	0.054(3)	0.001
C3−C4	0.051	0.053(3)	0	0.051	0.053(3)	0
Si−C7	0.051	0.052(3)	0	0.051	0.052(3)	0
C7−C23	0.046	0.047(3)	0.001	0.046	0.047(3)	0.001
C23−C22	0.045	0.047(3)	0	0.045	0.046(3)	0
C2−H	0.077	0.078(3)	0.002	0.077	0.078(3)	0.02

[a]Vibrational corrections lower than 0.001 are displayed as 0.
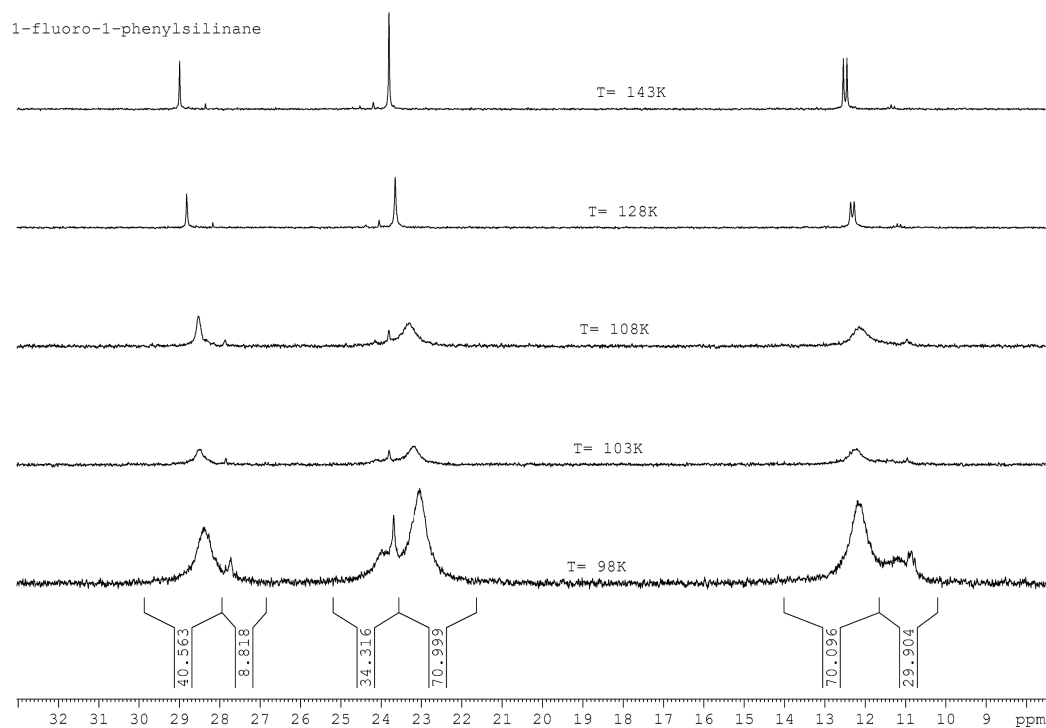
Figure 8. Variable-temperature ^{13}C NMR spectra of compound **3** in a Freon mixture (CD$_2$Cl$_2$:CHFCl$_2$:CHF$_2$Cl = 1:1:3): aliphatic carbon atoms C-2,6, C-3,5, and C-4, respectively.

taking the preferred equatorial position in 1,1-disubstituted silacyclohexane.

The assignment of the ^{13}C NMR signals to the conformers of compounds **3** and **4** is in complete agreement with earlier
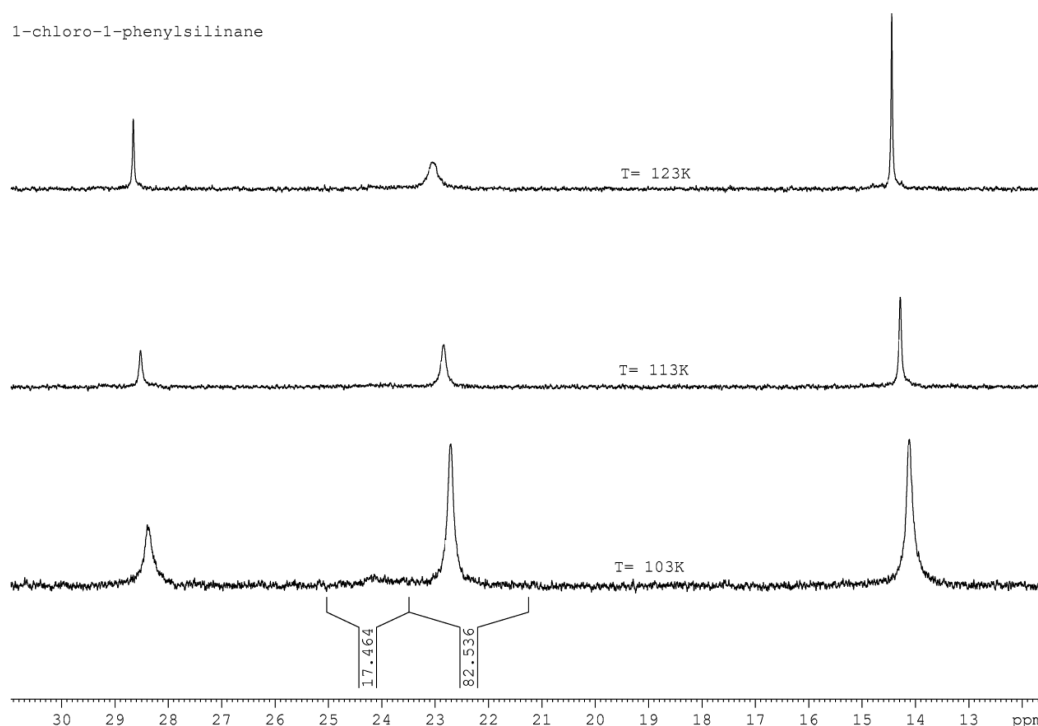
Figure 9. Variable-temperature ^{13}C NMR spectra of compound **4** in a Freon mixture (CD$_2$Cl$_2$:CHFCl$_2$:CHF$_2$Cl = 1:1:3): aliphatic carbon atoms C-2,6, C-3,5, and C-4, respectively.

results and with general stereochemical principles (e.g., the γ effect of axial substituents[35] on C-3,5 in ^{13}C NMR spectroscopy)[38] and was additionally checked by DFT/MP2 calculations of chemical shifts (Figures S3 and S4 in the Supporting Information).

■ DISCUSSION

Geometry. The calculated geometry is in good agreement with the electron diffraction results. Both theory and experiment show that the axial Si–X or Si–C$_{Ph}$ bonds are 0.005 Å longer than the corresponding equatorial bonds (Tables 1 and 2). This may be attributed to the σ(C2/6–H12/16)→σ*(Si–X) hyperconjugation, most pronounced for the anti location of the interacting orbitals. In comparison with the 1-phenyl-1-silacyclohexane molecule,[39,40] electronegative F and Cl atoms cause shortening of the neighboring Si–C2 and Si–C7 bonds by 0.011–0.021 Å. This may be rationalized by the relation between hybridization and electronegativity (Bent's rule[41]). This rule states that the s character concentrates in orbitals directed toward electropositive substituents or that atoms direct hybrid orbitals with more p character toward more electronegative elements. Therefore, the increase in the p character of the Si–X orbitals increases the s character of the orbitals of the immediately adjacent Si–C bonds, thus leading to their shortening. The Si–C7 bonds in **3** and **4** are about 0.02 Å shorter than the Si–C$_{Ph}$ bond in the PhSiMe$_3$ molecule.[42] Electropositive atoms, such as Si, cause a decrease in the ipso bond angle of the benzene ring from the regular hexagonal value of 120° to 117.1–118.4° (Tables 1 and 2). This is a known specific feature of molecules containing electropositive atoms connected to a phenyl group.[42]

Conformer Energies and Populations. As shown in Table 1, M06-2X calculations predict conformer **3**-Ph$_{eq}$ to be 0.3 kcal/mol more stable than **3**-Ph$_{axo}$, whereas MP2 calculations indicate that it is 0.5 kcal/mol less stable. The

third even less stable conformer is **3**-Ph$_{axi}$. The molecular graphs of the molecules under study are shown in Figures S1 and S2 in the Supporting Information. In **3**-Ph$_{axi}$, the H–H bond trajectories with the bond critical points (in green) are present between the H24 atom of the phenyl group and the axial hydrogen atoms H14 and H18 in positions 3 and 5, respectively, of the silacyclohexane ring. The H–H bond trajectories form a new pseudoring with the corresponding ring critical point (in red). The H–H interaction exhibits the characteristics of closed-shell interactions,[43] such as a low value of the electron density at the bond critical point (ρ_{BCP} = 0.006 au), relatively small positive values of the Laplacian ($\nabla^2\rho_{BCP}$ = 0.02 au), and close to zero reduced density gradient (RDG) values[23] (Figure S1). The fact that **3**-Ph$_{axi}$ is in an equilibrium state means that there are attractive forces acting on the hydrogen atoms linked by the H–H bond path.[44] On the other hand, the existence of the ring critical point in close proximity indicates that interactions of these hydrogen atoms are determined by a subtle balance of attractive and repulsive forces (green and orange regions, respectively; see Figure S1). As shown in Table 5, the phenyl group is 0.63 kcal/mol more stable in **3**-Ph$_{axi}$, whereas the silacyclohexane ring is more stable in **3**-Ph$_{eq}$ by 4.3 kcal/mol. In conformer **3**-Ph$_{axi}$, the main source of the silacyclohexane ring destabilization is the silicon atom. The axial protons at C3 (H14) and C5 (H18) in conformer **3**-Ph$_{axi}$ are more stable by 3.31 kcal/mol. The H24 atom of the phenyl group in this conformer, which points toward H14 and H18 atoms of the silacyclohexane ring, is at least 5.1 kcal/mol more stable than four other aromatic hydrogens. From the viewpoint of chemical intuition, for such location of the phenyl group, a repulsion could be expected, since the H24···H14(18) distance of 2.353 Å (M06-2X) is slightly less than the sum of the van der Waals radii of hydrogen atoms; however, the atoms involved are surprisingly stabilized. The H24 atom of the phenyl group in conformer **3**-Ph$_{eq}$, which

Table 5. M06-2X/cc-pvTZ Atomic and Molecular Energies of Conformers 3-Ph$_{axi}$ and 3-Ph$_{eq}$ (au) and Energy Differences (Δ, kcal/mol)

Aatom	3-Ph$_{axi}$	3-Ph$_{eq}$	Δ
Si1	−288.97264	−288.97955	4.34
C2	−38.26990	−38.27153	1.02
C3	−37.94257	−37.94370	0.71
C4	−37.96636	−37.96498	−0.86
C5	−37.94240	−37.94365	0.78
C6	−38.26982	−38.27144	1.02
F8	−100.28174	−100.27736	−2.75
Hax(C3)	−0.64160	−0.63632	−3.31
Heq(C3)	−0.63886	−0.63998	0.71
Hax(C5)	−0.64164	−0.63633	−3.33
Heq(C5)	−0.63892	−0.63998	0.67
Hax(C2)	−0.62137	−0.62379	1.52
Heq(C2)	−0.62062	−0.61946	−0.73
Hax(C6)	−0.62142	−0.62371	1.44
Heq(C6)	−0.62062	−0.61946	−0.73
Hax(C4)	−0.63750	−0.63915	1.03
Heq(C4)	−0.63888	−0.63895	0.04
H24	−0.62754	−0.62470	−1.78
H25	−0.61941	−0.61916	−0.16
H26	−0.61891	−0.61887	−0.02
H27	−0.61882	−0.61865	−0.11
H28	−0.61436	−0.61434	−0.01
$\sum_\Omega E(\Omega)$	−817.60386	−817.60533	0.92
SCF energy	−817.60384	−817.60513	0.81
$\sum_\Omega E(\Omega)$ SCF	−0.01	−0.12	0.11
Si ring	−485.68512	−485.69197	4.30
Ph ring	−231.63701	−231.63600	−0.63

Table 6. M06-2X/cc-pvTZ Atomic and Molecular Energies of Conformers 4-Ph$_{axo}$ and 4-Ph$_{eq}$ (au) and Energy Differences (Δ, kcal/mol)

Atom	4-Ph$_{axo}$	4-Ph$_{eq}$	Δ
Si1	−288.80721	−288.81232	3.20
C2	−38.21636	−38.21596	−0.25
C3	−37.89741	−37.89753	0.07
C4	−37.91596	−37.91589	−0.05
C5	−37.89723	−37.89745	0.14
C6	−38.21663	−38.21624	−0.25
Cl8	−461.32863	−461.32660	−1.28
Hax(C3)	−0.63481	−0.63378	−0.64
Heq(C3)	−0.63835	−0.63957	0.76
Hax(C5)	−0.63749	−0.63382	−2.30
Heq(C5)	−0.63830	−0.63961	0.82
Hax(C2)	−0.62043	−0.62322	1.75
Heq(C2)	−0.62113	−0.61811	−1.89
Hax(C6)	−0.61914	−0.62319	2.54
Heq(C6)	−0.62178	−0.61813	−2.29
Hax(C4)	−0.63708	−0.63887	1.12
Heq(C4)	−0.63853	−0.63873	0.12
H24	−0.62353	−0.62545	1.21
H25	−0.61917	−0.61921	0.03
H26	−0.61867	−0.61894	0.17
H27	−0.61868	−0.61876	0.05
H28	−0.62032	−0.61357	−4.24
$\sum_\Omega E(\Omega)$	−1177.94129	−1177.94299	1.07
SCF energy	−1177.94151	−1177.94270	0.74
$\sum_\Omega E(\Omega)$ SCF	0.14	−0.18	0.32
Si ring	−946.58647	−946.58901	1.59
Ph ring	−231.35481	−231.35398	−0.52

points to the center of the silacyclohexane ring, is at least 3.5 kcal/mol more stable than four other aromatic hydrogens and 1.8 kcal/mol less stable than the H24 atom of the 3-Ph$_{axi}$ conformer. The fluorine atom destabilizes conformer 3-Ph$_{eq}$ by 2.8 kcal/mol. Similar relations are observed in conformers 4-Ph$_{axo}$ and 4-Ph$_{eq}$ (Table 6).

The strong axial preference of electronegative groups at silicon[12−16] and the known values of the conformational energies A ($A = G_{ax} − G_{eq}$) for the fluorine atom (−0.28),[16] chlorine atom (−0.43),[17] and the phenyl group (0.25 kcal/mol),[2] taking into account the additivity of conformational energies of the substituents at silicon,[2] all suggest the predominance of the Ph$_{eq}$ conformers for compounds 3 and 4. Indeed, for the chloro derivative 4, both experiment (NMR, GED) and theory (MP2, M06-2X) give the predominance of 4-Ph$_{eq}$ conformer with the equilibrium constant K for the conformational equilibrium 4-Ph$_{ax}$ ⇆ 4-Ph$_{eq}$ equal to 4.7 (LT NMR), 3.8 (GED), or 2.4 (M06-2X). More complex is the situation with the fluoro derivative 3. The LT NMR measurements, again, give the predominance of 3-Ph$_{eq}$ conformer at the very low temperature of 98 K, the K value of 3.0−3.3 being lower in compliance with the smaller axial preference of fluorine with respect to chlorine. The M06-2X calculations also predict the predominance of 3-Ph$_{eq}$ (Δ$G°$ = 0.7 kcal/mol), but MP2 calculations show the value of ΔE for 3-Ph$_{eq}$ to be 0.5 kcal/mol higher than that for 3-Ph$_{ax}$ (Table 1). Frequency calculations could not be performed at the MP2/aug-cc-pVTZ level of theory, but a comparison of the ΔE and Δ$G°$ values obtained at the M06-2X/aug-cc-pVTZ level allows us to conclude that taking into account the entropy term makes

the 3-Ph$_{eq}$ conformer more favorable by 0.4 kcal/mol (Table 1). Therefore, considering the entropy term would make the MP2 value of Δ$G°$ close to 0 and, thus, the populations of the 3-Ph$_{eq}$ and 3-Ph$_{ax}$ conformers are almost equal. From the GED experiment, taking into account the error bars, the molar ratio of the 3-Ph$_{axi}$ and 3-Ph$_{eq}$ conformers is close to unity. Apart from solvation effects, the different ratios of the conformers measured by the LT NMR and GED can be partially due to the very different temperatures of measurements in the two methods: an increase of the temperature increases the relative fraction of the less stable Ph$_{ax}$ conformer.

To summarize, the molecules of 1-chloro-1-phenyl-1-silacyclohexane (4) exist both in the gas phase and in solution predominantly in the 4-Ph$_{eq}$ conformation, as proved both experimentally and theoretically by electron diffraction, low-temperature NMR, and M06-2X and MP2 quantum chemical calculations. Its fluorine analogue, 1-fluoro-1-phenyl-1-silacyclohexane (3), in solution also gives an equilibrium mixture, although the predominance of the 3-Ph$_{eq}$ conformer is less pronounced in compliance with less negative conformational energies A for fluorine in comparison to those for chlorine.[16,17] The observed conformational preferences are nicely reproduced by DFT (M06-2X) calculations, whereas the MP2 method predicts 3-Ph$_{eq}$ to be *energetically* less stable. Indirect consideration of the entropy contribution suggests a close to 0 value of the *free energy* difference Δ$G°$ for the conformers of 3. The shift of the conformational equilibrium to more stable species is apparently also responsible for the higher content of the Ph$_{eq}$ conformers in the low-temperature NMR experiments in comparison to room-temperature GED measurements.

ASSOCIATED CONTENT

Ⓢ Supporting Information

The Supporting Information is available free of charge on the ACS Publications website at DOI: 10.1021/acs.joc.6b02538.

Conditions of synchronous GED/MS experiments, topological analysis for the conformers of **3** and **4**, *xyz* files of atomic Cartesian coordinates and energies of all optimized structures, and atomic charges and calculated ^{13}C chemical shifts (PDF)

AUTHOR INFORMATION

Corresponding Authors

*E-mail for B.A.S.: bagrat@irioch.irk.ru.
*E-mail for A.V.B.: belyakov@lti-gti.ru.
*E-mail for E.K.: ekleinp@uni-potsdam.de.

ORCID Ⓞ

Bagrat A. Shainyan: 0000-0002-4296-7899

Notes

The authors declare no competing financial interest.

ACKNOWLEDGMENTS

REFERENCES

(1) Shainyan, B. A. Structure and Conformational Analysis of Silacyclohexanes and 1,3-Silaheterocyclohexanes. *Tetrahedron* **2016**, *72*, 5027−5035.

(2) Shainyan, B. A.; Kleinpeter, E. Conformational Preferences of Si-Ph,H and Si-Ph,Me Silacyclohexanes and 1,3-Thiasilacyclohexanes. Additivity of Conformational Energies in 1,1-Disubstituted Heterocyclohexanes. *Tetrahedron* **2012**, *68*, 114−125.

(3) Wallevik, S. Ó.; Bjornsson, R.; Kvaran, Á.; Jonsdottir, S.; Girichev, G. V.; Giricheva, N. I.; Hassler, K.; Arnason, I. Conformational properties of 1-fluoro-1-methyl-silacyclohexane and 1-methyl-1-trifluoromethyl-silacyclohexane: Gas electron diffraction, low-temperature NMR, temperature-dependent Raman spectroscopy, and quantum chemical calculations. *J. Mol. Struct.* **2010**, *978*, 209−219.

(4) Klaeboe, P.; Nielsen, C. J.; Horn, A.; Guirgis, G. A.; Overby, J. S.; Aleksa, V. Raman and infrared spectra, quantum chemical calculations, conformations and spectral assignments of 1-chloro-1-methyl-1-silacyclohexane. *J. Mol. Struct.* **2013**, *1047*, 282−291.

(5) Kern, T.; Hölbling, M.; Dzambaski, A.; Flock, M.; Hassler, K.; Wallevik, S. Ó.; Arnason, I.; Bjornsson, R. Conformational energies of silacyclohexanes $C_5H_{10}SiHMe$, $C_5H_{10}SiH(CF_3)$ and $C_5H_{10}SiCl(SiCl_3)$ from variable temperature Raman spectra. *J. Raman Spectrosc.* **2012**, *43*, 1337−1342.

(6) Shainyan, B. A.; Kirpichenko, S. V.; Kleinpeter, E. Synthesis and conformational analysis of 1,3- azasilinanes. *Tetrahedron* **2012**, *68*, 7494−7501.

(7) Shainyan, B. A.; Kirpichenko, S. V.; Kleinpeter, E. Synthesis and conformational properties of 1,3-dimethyl-3-phenyl-1,3-azasilinane. Low temperature dynamic NMR and computational study. *Arkivoc* **2012**(v), 175−185.

(8) Kirpichenko, S. V.; Shainyan, B. A.; Kleinpeter, E. Unusual conformational preferences of 1,3-dimethyl-3-isopropoxy-3-silapiperidine. *J. Phys. Org. Chem.* **2012**, *25*, 1321−1327.

(9) Shainyan, B. A.; Kirpichenko, S. V.; Kleinpeter, E.; Shlykov, S. A.; Osadchiy, D. Yu. Molecular structure and conformational analysis of 3-methyl-3-phenyl-3-silatetrahydropyran. Gas-phase electron diffraction, low temperature NMR and quantum chemical calculations. *Tetrahedron* **2015**, *71*, 3810−3818.

(10) Shainyan, B. A.; Kirpichenko, S. V.; Kleinpeter, E. Stereochemistry of 3-isopropoxy-3-methyl-1,3-oxasilinane − the first 3-silatetrahedropyran with an exocyclic RO−Si bond. *Tetrahedron* **2015**, *71*, 6720−6726.

(11) Kirpichenko, S. V.; Kleinpeter, E.; Ushakov, I. A.; Shainyan, B. A. Conformational analysis of 3-methyl-3-silathiane and 3-fluoro-3-methyl-3-silathiane. *J. Phys. Org. Chem.* **2011**, *24*, 320−326.

(12) Girichev, G. V.; Giricheva, N. I.; Bodi, A.; Gudnason, P. I.; Jonsdottir, S.; Kvaran, A. I.; Arnason, I.; Oberhammer, H. Unexpected conformational properties of 1-trifluoromethyl-1-silacyclohexane, $C_5H_{10}SiHCF_3$: gas electron diffraction, low-temperature NMR spectropic studies, and quantum chemical calculations. *Chem. - Eur. J.* **2007**, *13*, 1776−1783.

(13) Belyakov, A. V.; Baskakov, A. A.; Naraev, V. N.; Rykov, A. N.; Oberhammer, H.; Arnason, I.; Wallevik, S. O. Molecular structure and conformational preferences of 1-chloro-1-silacyclohexane, $CH_2(CH_2CH_2)_2SiH−Cl$, as studies by gas-phase electron diffraction and quantum chemistry. *Russ. J. Gen. Chem.* **2011**, *81*, 2257−2261.

(14) Shainyan, B. A.; Kirpichenko, S. V.; Kleinpeter, E.; Shlykov, S. A.; Osadchiy, D.; Yu; Chipanina, N. N.; Oznobikhina, L. P. 1,3-Dimethyl-3-silapiperidine: synthesis, molecular structure, and conformational analysis by gas-phase electron diffraction, low temperature NMR, IR and Raman spectroscopy, and quantum chemical calculations. *J. Org. Chem.* **2013**, *78*, 3939−3947.

(15) Belyakov, A. V.; Baskakov, A. A.; Naraev, V. N.; Rykov, A. N.; Oberhammer, H.; Arnason, I.; Wallevik, S. O. Molecular Structure and Conformational Preferences of 1-Bromo-1-Silacyclohexane, $CH_2(CH_2CH_2)_2SiH−Br$, as Studied by Gas-Phase Electron Diffraction and Quantum Chemistry. *Russ. J. Phys. Chem. A* **2012**, *86*, 1563−1566.

(16) Bodi, A.; Kvaran, A.; Jonsdottir, S.; Antonsson, E.; Wallevik, S. O.; Arnason, I.; Belyakov, A. V.; Baskakov, A. A.; Hölbling, M.; Oberhammer, H. Conformational properties of 1-fluoro-1-silacyclohexane, $C_5H_{10}SiHF$: gas electron diffraction, low temperature NMR, and quantum chemical calculations. *Organometallics* **2007**, *26*, 6544−6550.

(17) Wallevik, S. Ó.; Bjornsson, R.; Kvaran, Á.; Jonsdottir, S.; Arnason, I.; Kern, T.; Hassler, K. Conformational Properties of 1-Halogenated-1-Silacyclohexanes, C5H10SiHX (X = Cl, Br, I): Gas Electron Diffraction, Low-Temperature NMR, Temperature-Dependent Raman Spectroscopy, and Quantum-Chemical Calculations. *Organometallics* **2013**, *32*, 6996−7005.

(18) Eliel, E. I.; Manoharan, M. Conformational analysis. 40. Conformation of 1-methyl-1-phenylcyclohexane and conformational energies of the phenyl and vinyl groups. *J. Org. Chem.* **1981**, *46*, 1959−1962.

(19) Wiberg, K. B.; Castejon, H.; Bailey, W. F.; Ochterski, J. Conformational studies in the cyclohexane series. 2. Phenylcyclohexane and 1-methyl-1-phenylcyclohexane. *J. Org. Chem.* **2000**, *65*, 1181−1187.

(20) Suslova, E. N.; Shainyan, B. A. 1-Phenyl-1-halo-1-silacyclohexanes. *Russ. J. Gen. Chem.* **2016**, *86*, 1854−1858.

(21) Frisch, M. J.; Trucks, G. W.; Schlegel, H. B.; Scuseria, G. E.; Robb, M. A.; Cheeseman, J. R.; Scalmani, G.; Barone, V.; Mennucci, B.; Petersson, G. A.; Nakatsuji, H.; Caricato, M.; Li, X.; Hratchian, H. P.; Izmaylov, A. F.; Bloino, J.; Zheng, G.; Sonnenberg, J. L.; Hada, M.; Ehara, M.; Toyota, K.; Fukuda, R.; Hasegawa, J.; Ishida, M.; Nakajima, T.; Honda, Y.; Kitao, O.; Nakai, H.; Vreven, T.; Montgomery, J. A., Jr.; Peralta, J. E.; Ogliaro, F.; Bearpark, M.; Heyd, J. J.; Brothers, E.; Kudin, K. N.; Staroverov, V. N.; Keith, T.; Kobayashi, R.; Normand, J.; Raghavachari, K.; Rendell, A.; Burant, J. C.; Iyengar, S. S.; Tomasi, J.; Cossi, M.; Rega, N.; Millam, J. M.; Klene, M.; Knox, J. E.; Cross, J. B.; Bakken, V.; Adamo, C.; Jaramillo, J.; Gomperts, R.; Stratmann, R. E.; Yazyev, O.; Austin, A. J.; Cammi, R.; Pomelli, C.; Ochterski, J. W.; Martin, R. L.; Morokuma, K.; Zakrzewski, V. G.; Voth, G. A.; Salvador, P.; Dannenberg, J. J.; Dapprich, S.; Daniels, A. D.; Farkas, O.; Foresman, J. B.; Ortiz, J. V.; Cioslowski, J.; Fox, D. J. *Gaussian 09*, *revision D01*; Gaussian, Inc., Wallingford, CT, 2013.

(22) Bader, R. F. W. *Atoms in Molecules: A Quantum Theory*; Oxford University Press: New York, 1994.

(23) Johnson, E. R.; Keinan, S.; Mori-Sánchez, P.; Contreras-García, J.; Cohen, A. J.; Yang, W. Revealing noncovalent interactions. *J. Am. Chem. Soc.* **2010**, *132*, 6498−6506.

(24) Contreras-García, J.; Johnson, E. R.; Keinan, S.; Chaudret, R.; Piquemal, J.-P.; Beratan, D. N.; Yang, W. NCIPLOT: a program for plotting noncovalent interaction regions. *J. Chem. Theory Comput.* **2011**, *7*, 625−632.

(25) Girichev, G. V.; Shlykov, S. A.; Petrova, V. N.; Subbotina, N. Y.; Lapshina, S. B.; Danilova, T. G. *Izv. Vyssh. Uchebn. Zaved., Khim. Khim. Tekhnol.* **1988**, *31*, 46 (in Russian).

(26) Girichev, G. V.; Shlykov, S. A.; Revichev, Y. F. *Prib. Tekh. Eksp.* **1986**, *4*, 167 (in Russian).

(27) Girichev, G. V.; Utkin, A. N.; Revichev, Y. F. *Prib. Tekh. Eksp.* **1984**, *2*, 187 (in Russian).

(28) Girichev, E. G.; Zakharov, A. V.; Girichev, G. V.; Bazanov, M. V. *Izv. Vyssh. Uchebn. Zaved., Technol. Tekstil. Prom.* **2000**, *2*, 142−146 (in Russian).

(29) Ross, A. W.; Fink, M.; Hilderbrandt, R. L. In *International tables for crystallography*; Kluwer Academic: Dordrecht, The Netherlands, 1992.

(30) Hilderbrandt, R. L. Cartesian coordinates of molecular models. *J. Chem. Phys.* **1969**, *51*, 1654−1659.

(31) Andersen, B.; Seip, H. M.; Strand, T. G.; Stolevik, R. Procedure and computer programs for the structure determination of gaseous molecules from electron diffraction data. *Acta Chem. Scand.* **1969**, *23*, 3224−3234.

(32) Gundersen, G.; Samdal, S.; Seip, H. M. *Least squares structural refinement program based on gas electron-diffraction data*; Department of Chemistry, University of Oslo: Oslo, Norway, 1981; Parts I−III.

(33) Vishnevskiy, Y. V. The initial processing of the gas electron diffraction data: New method for simultaneous determination of the sector function and electron wavelength from gas standard data. *J. Mol. Struct.* **2007**, *871*, 24−32.

(34) Sipachev, V. A. Vibrational effects in diffraction and microwave experiments: A start on the problem. In *Advances in molecular structure research*; Hargittai, I., Hargittai, M., Eds.; JAI Press: New York, 1999.

(35) Sipachev, V. A. Calculation of shrinkage corrections in harmonic approximation. *J. Mol. Struct.: THEOCHEM* **1985**, *121*, 143−151.

(36) Shainyan, B. A.; Kleinpeter, E. *Tetrahedron* **2013**, *69*, 5927−5936.

(37) Arnason, I.; Kvaran, A.; Jonsdottir, S.; Gudnason, P. I.; Oberhammer, H. Conformations of silicon-containing rings. 5. Conformational properties of 1-methyl-1-silacyclohexane: gas electron diffraction, low-temperature NMR, and quantum chemical calculations. *J. Org. Chem.* **2002**, *67*, 3827−3831.

(38) Aleksa, V.; Guirgis, G. A.; Horn, A.; Klaeboe, P.; Liberatore, R. J.; Nielsen, C. *Vib. Spectrosc.* **2012**, *61*, 167−175.

(39) Kleinpeter, E. *Adv. Heterocycl. Chem.* **2004**, *86*, 41−126.

(40) Shainyan, B. A.; Kirpichenko, S. V.; Osadchiy, D. Y.; Shlykov, S. A. *Struct. Chem.* **2014**, *25*, 1677−1685.

(41) Bent, H. A. An Appraisal of Valence-bond Structures and Hybridization in Compounds of the First-row elements. *Chem. Rev.* **1961**, *61*, 275−311.

(42) Campanelli, A. R.; Ramondo, F.; Domenicano, A.; Hargittai, I. Molecular structure and conformation of trimethylsilylbenzene: a study by gas-phase electron diffraction and theoretical calculations. *J. Organomet. Chem.* **1997**, *536-537*, 309−318.

(43) Bader, R. F. W.; Essén, H. The characterization of atomic interactions. *J. Chem. Phys.* **1984**, *80*, 1943−1960.

(44) Matta, C. F.; Hernandez-Trujillo, J.; Tang, T.-H.; Bader, R. F. W. Hydrogen-Hydrogen Bonding: A Stabilizing Interaction in Molecules and Crystals. *Chem. - Eur. J.* **2003**, *9*, 1940−1951.